Estimation of Gaze from EEG for Cursor Control

article published on www.hakenberg.de in 2011

***Abstract*—The variations in the electrooculogram (EOG) caused by eye motion are roughly proportional to the instantaneous horizontal and vertical glance angle. This simple linear correlation is exploited in systems using EOG to control software, and hardware such as artificial limbs, or wheelchairs. The drift in the electronics is commonly compensated for by applying a high-pass filter. Consequently, the remaining EOG signal contains only blinks and rapid eye movement. However, repeating these eye gestures voluntarily is exhausting. Our paper presents an algorithm that estimates the instantaneous glance of a subject, who wears an EEG cap. The subject is seated in front of a computer screen in order to control an application by glance. Because the visual field of interest, in this setting, is the limited area of the monitor, we can compensate the error in the glance estimate by detecting outliers. Because no high-pass filter is applied to the data, the user controls applications simply by glance, which is comfortable even over extended periods of time. The numerical evaluation of the experiments with 12 volunteers, and video recordings of EOG controlled applications demonstrate the accuracy of our algorithm.**

***Index Terms*—Electrooculography, Electroencephalography, Human computer interaction.**

I. Introduction

THE front and the back of the human eye sustain an electric potential difference. The potentials propagate to the cheeks, forehead, and scalp, where electrooculogram (EOG), or electroencephalogram (EEG) electrodes can pick them up. A reorientation of the eyes generally causes a change in the voltages measured by the electrodes.

Whereas the signal patterns originating from eye movement are undesired in applications that monitor brain activity, the patterns constitute a reliable means of control in an EOG based human-machine interface. A person without correct limb and facial muscular control might still have the ability to gesture through eye movement and blinks. Diseases such as amyotrophic lateral sclerosis, or certain forms of quadriplegic clinical conditions (spinal cord injury, locked-in syndrom) render patients with as little forms of expression as blinking and orienting the eyes. Automating the interpretation of these gestures can lead to a more autonomous lifestyle and increased quality of life [1, 2].

Researchers have been particularly successful at detecting eye blinks in the EOG, and classifying oscillatory eye movements, i.e. sequences of glance directions, for example ”left-right-center” that are performed over a few seconds. Consequently, these eye gestures would operate a wheelchair [1], a robot [3], or software for spelling words, and express needs in a home environment [4-6]. In the future, psychological research, gaming electronics, consumer electronics, and the long term examination of eye movements might result in more

This research was funded by the Curtin Strategic International Research Scholarship and the Institute for Infocomm Research through A*STAR.

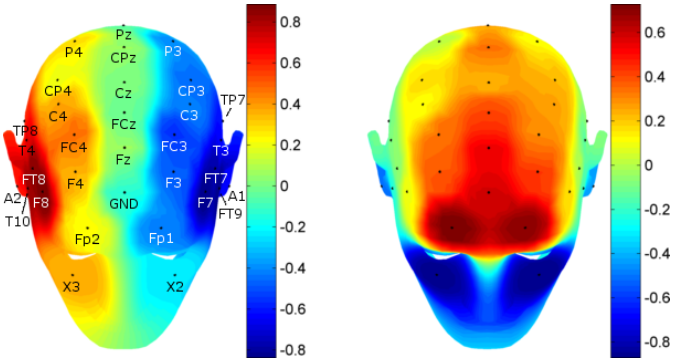

Fig. 1. Linear correlation coefficients of channel measurements with horizontal (left) and vertical (right) glance direction averaged for 12 subjects as presented in [14]. The reference electrode is Oz at the back of the head. Values of ± 1 would indicate a perfect linear correlation. The black dots indicate the location of electrodes between which the values are interpolated.

applications [7]. Compared to video-based eye trackers, EOG is independent of lighting conditions and also works when the eye lids are closed [8]. Besides, EOG is used to remove ocular artifacts from EEG to unveil brain activity, see [9] for references. The technique presented in our paper does not categorize as brain computer interface as the control is not based on the classification of brain activity.

Common within the literature on EOG-based control is the application of a high-pass filter, with cutoff at a frequency between 0.05 and 0.2 Hz. The high-pass filter removes the long-term drift inherent in all channels that are connected to the scalp, [10]. Over short periods of time, typically less than 10 seconds, the drift is negligible given that the subject is at rest. During this phase, the variation in EOG is nearly colinear to the glance angle within the customary field of view [11, 12], thus linear regression as defined in (1) reliably transforms EOG to glance direction. However, since the EOG-based control is required to operate for extended periods of time, researchers have relied on the classification of oscillatory eye movements from the high-pass filtered data. One exception is [3], who performs periodic recalibrations: To reset the positional control, the user ”fixates on a direct forward gaze for approximately 1/2 second, then blinks.” Another approach is presented in [13], that fits the measured velocity profile of the EEG during a saccade to the average velocity profile during a standard saccade in order to integrate the eye rate over time to the glance direction.

Our new approach is motivated by two observations:

1) the majority of EOG-controlled applications are displayed on a computer screen to provide feedback with the shortest amount of delay possible. When the glance is falsely estimated to lie outside of the screen area, a simple translation can account for the offset. Drift is

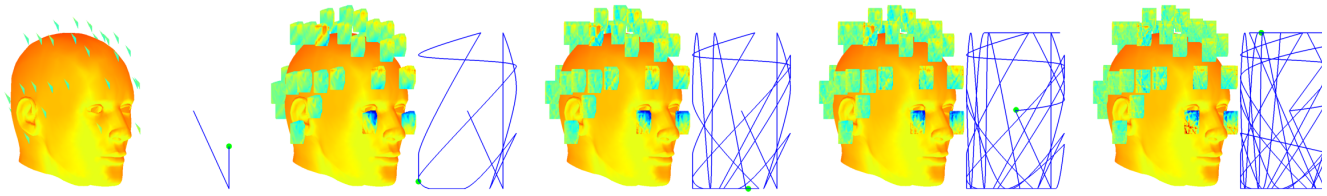

Fig. 2. The cascade visualizes the accumulation of EEG at intervals of 15 seconds as the eyes track the cue that moves along the curve. At each location of the 36 electrodes the voltage is mapped within a square domain at the coordinate corresponding to the cue position.

corrected on the fly.

2) activities such as reading, and watching a movie are comfortably performed over extended periods of time, during which the glance targets the changing region of interest, while blinks occur infrequently and involuntarily. Any EOG-based application that creates the incentive for the same behavioural pattern, is likely to have low fatiguing effect. Until now, most applications are based on voluntary blinks and oscillation of glance.

The paper is organized as follows: We advocate the use of a linear model to estimate eye orientation from raw EEG data. No filtering is required. The subject- and session specific model is obtained from a short calibration procedure. In order to accurately estimate the glance over extended periods of time (typically more than 10 minutes) on a computer screen, we introduce a drift compensation that translates outliers back onto the screen. A simple computation reveals that our algorithm is potentially invariant under arbitrary shift of baselines. From the trials with 12 volunteers, we conclude that our estimation is generally faithful within a tolerance of 5 cm in horizontal and vertical direction. Finally, we report on two conventional applications that were successfully controlled by a subject wearing an EEG cap using our algorithm.

II. Method

A. Model

Voltage gradients measured from skin around the eyes exhibit a nearly perfect linear correlation with the glance ranging within $\pm 45°$ for left-right and within $\pm 30°$ for up-down direction [12]. For electrodes further away, located on the scalp, the correlation coefficients were studied in [14] and are reproduced in Figure 1. For instance, electrodes on the temples correlate significantly with the left-right glance, whereas channels located along the centerline of the scalp exhibit a significant correlation with the up-down glance. Our model to estimate the glance from EEG exploits the cumulative linear correlation with the vertical and horizontal glance direction of all connected channels.

We assume the EEG amplifier provides the number of n channels, which are referenced to a ground electrode. For each channel $i = 1, 2, \ldots, n$, the measured EEG signal m_i is the sum of the effect of the glance g_i, and a remaining signal component c_i that is composed of 1) a channel specific, drifting baseline, 2) potential fluctuation induced by brain activity, as well as 3) noise. The contributions of 2) and 3) are of significantly lower amplitude than the glance g_i and have zero mean. We write $m_i = g_i + c_i$ for $i = 1, 2, \ldots, n$.

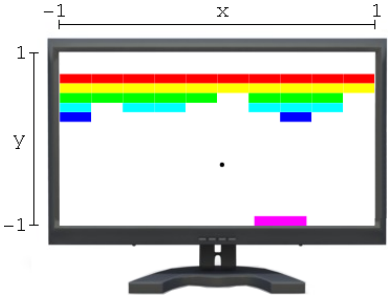

Fig. 3. Coordinate system of the monitor, with the game *Breakout* displayed on the screen

A computer screen is placed in front of the subject as close as possible given that the glance can still be comfortably directed into all corners of the screen. Let $p = (x, y)$ denote the coordinate on the screen towards which the glance is directed. The coordinate system $-1 \leq x, y \leq 1$ is indicated in Figure 3. The contribution of the glance g_i on channel $i = 1, 2, \ldots, n$ is modeled as $g_i(p) = \beta_i^x \cdot x + \beta_i^y \cdot y$ where β_i^x, β_i^y are related to the coefficients shown in Figure 1.

B. Calibration

During the calibration procedure of duration T, the subject is required to visually trace a moving cue at coordinate $p(t) = (x(t), y(t))$ on the computer screen while moving the head as little as possible. Subsequent to the calibration procedure, the system tolerates turning and tilting of the head quite successfully due to our way of drift handling. Because of linearity, we express the correlation of the measurements m_i and the glance direction (x, y) at time t simply by the matrix multiplication

$$\begin{pmatrix} m_1 & m_2 & \cdots & m_n & 1 \end{pmatrix} \begin{pmatrix} \alpha_1^x & \alpha_1^y \\ \alpha_2^x & \alpha_2^y \\ \vdots & \vdots \\ \alpha_n^x & \alpha_n^y \\ \alpha_0^x & \alpha_0^y \end{pmatrix} = \begin{pmatrix} x & y \end{pmatrix} \tag{1}$$

The EEG collected during the calibration procedure from $t = 0, \ldots, T$, and the coordinates of the cue upsampled to the rate of the EEG compile into an overdetermined system of linear equations. The unknowns α_i^x, α_i^y for $i = 0, 1, 2, \ldots, n$ are solved for by minimizing the squared error in (1). The purpose of the coefficients α_0^x, α_0^y is to compensate the baseline offset in all channels. Figure 2 symbolizes the calibration procedure at different points in time.

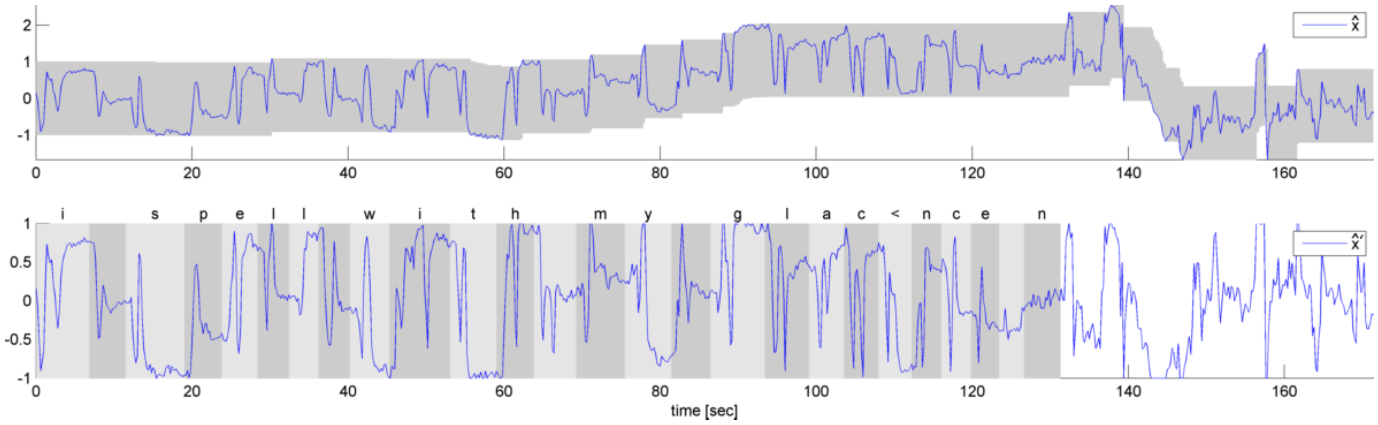

Fig. 4. Glance estimation $\hat{x}$ over a period of 3 minutes (top), and mapped to the interval $[-1, 1]$ results in the final glance estimation $\hat{x}'$ (bottom).

The synchronization of the EEG m_i with the cue position p on the screen are crucial in (1). Common practice is to send trigger pulses to the amplifier via serial port messaging. However, there remains a bias that depends on the graphics system: A single LCD screen might respond faster than a stereo display. So instead, we mount a photodiode circuit in front of the display to determine the lag between vision and EEG. The circuit consists of a photodiode, and a resistor only, and feeds directly into one of the spare channels of the amplifier. Periodic flashes on the display beneath the photodiode result in pulses of 100μV amplitude, and give means of analog synchronization. Because we have used this design principle successfully to detect delicate P300 patterns, we are convinced that the EEG is not altered by connecting a weak active electronic component to the amplifier. The photodiode circuit is not required after calibration, as simply the most recent EEG available is used to estimate the glance direction.

C. Algorithm

Subsequent to the calibration procedure, we assume that the position $p = (x, y)$ of the glance on the monitor is unknown. However, having solved the linear system defined by (1), the coefficients α_i^x, α_i^x for $i = 0, 1, 2, \ldots, n$ are at hand to obtain an estimate $\hat{p} = (\hat{x}, \hat{y})$ using the most recent EEG data m_i. We simply evaluate

$$\begin{pmatrix} \hat{x} & \hat{y} \end{pmatrix} = \begin{pmatrix} m_1 & m_2 & \cdots & m_n & 1 \end{pmatrix} \begin{pmatrix} \alpha_1^x & \alpha_1^y \\ \alpha_2^x & \alpha_2^y \\ \vdots & \vdots \\ \alpha_n^x & \alpha_n^y \\ \alpha_0^x & \alpha_0^y \end{pmatrix} \tag{2}$$

Since the signal induced by brain activity as well as the noise are assumed to have zero mean, these contributions are conveniently annihilated by averaging the results of (2) for measurements m_i of the most recent 0.1 sec.

As discussed in [20], the measurements m_i might be subject to drift in the baselines. Consequently, the estimated position $\hat{p}$ is likely to be offset to the actual glance position after a short period of time. We make the assumption, that the subject's glance is directed to a point on the computer screen, thus, the estimated position should not be located outside the screen. As soon as (2) yields a coordinate $\hat{x}, \hat{y}$ outside the coordinate area of the screen $-1 \leq \hat{x}, \hat{y} \leq 1$, we introduce a correction by translating each coordinate back into the valid area with the minimum shift necessary. This corrective term is applied to subsequent estimations until the condition $-1 \leq \hat{x}, \hat{y} \leq 1$ is violated again.

The horizontal and vertical correction mechanisms are independent and identical, thus we only describe the compensation that corrects the horizontal glance estimation: We introduce a variable q^x to represent the offset of a window of view along the x-axis. Initially, we set $q^x = 0$. Instead of $\hat{x}$, we define $\hat{x}' = \hat{x} - q^x$ to be the estimated glance position on the screen. If during the process $\hat{x}'$ lies outside the screen, we simply update q^x. Specifically, if $\hat{x}' = \hat{x} - q^x < -1$, we redefine $q^x := \hat{x} + 1$. On the other hand, if $1 < \hat{x} - q^x$, we update $q^x := \hat{x} - 1$. With the modified value q^x the estimation $\hat{x}' = \hat{x} - q^x$ is guaranteed to be within the bounds of the screen coordinate system $[-1, 1]$. Analogous for q^y. The final glance estimate is defined as $\hat{p}' = (\hat{x}', \hat{y}')$.

Figure 4 shows an example how $\hat{x}$ and $\hat{x}'$ might evolve in practice.

D. Analysis

There are different circumstances that generally lead to a deterioration of the approximation (2): turning of the head, mimic, or drift in the electrodes. However, our experiments suggest that all of these artifacts can be compensated using the strategy above. In fact, a simple computation reveals that adding constant offsets δ_i to the measurements m_i for $i = 1, 2, \ldots, n$ can be compensated by our algorithm. Again, we demonstrate this only for the x-axis:

$$\alpha_0^x + \sum_{i=1}^{n} (m_i + \delta_i)\alpha_i^x = \underbrace{\alpha_0^x + \sum_{i=1}^{n} m_i \alpha_i^x}_{\hat{x}} + \underbrace{\sum_{i=1}^{n} \delta_i \alpha_i^x}_{c} = \hat{x} + c \tag{3}$$

and $\hat{x}' = \hat{x} + c - q^x$. By allowing for $q^x = c$, then $\hat{x}' = \hat{x} + c - c = \hat{x}$. Thus, adding constant offsets δ_i to m_i do not

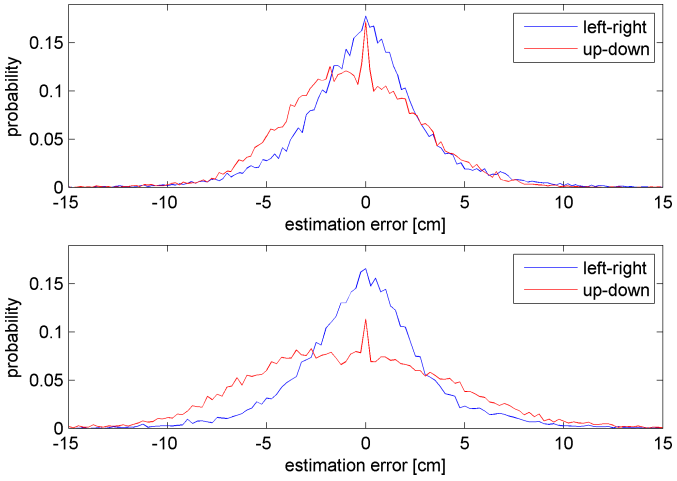

Fig. 5. Probability distribution of estimation error $e(t)$ averaged from 12 subjects. *Top:* Electrodes X2 and X3 are connected 2 cm below the eyes. *Bottom:* No electrodes below the eyes.

necessarily affect the estimation. The offsets δ_i represent the alterations in the baselines due to drift.

Remark: A higher than linear order approximation of the screen coordinates through terms such as m_i^2, m_i^3 in (1), spoils the unification of change in baselines into a single unknown $c = \sum_{i=1}^{n} \delta_i \alpha_i^x$. Therefore, the simple drift compensation carried out above does not trivially extend to higher order models. [20] uses a quadratic approximation, and omits drift compensation.

III. Experimental Results

A. Subjects and Materials

The following experiments have been approved by the human research ethics committee of Curtin University under the reference SMEC-18-10. Twelve subjects aged between 18 and 45 participated in the experiments voluntarily, after they had given written consent. They had the right to leave the recording session at any time. Their anonymity were guaranteed.

The subject is seated in front of a 22" monitor with a distance of 60 cm between forehead and screen. The screen is 47.3 cm wide and 29.7 cm high. Thus, the left-right glance angle ranges between $\pm 21.5°$, and the up-down glance angle is between $\pm 13.9°$.

To acquire the EEG, we use the 40 channel monopolar digital amplifier NuAmps of which $n = 36$ channels are effectively connected to the subject. Optionally, two additional EOG electrodes labeled X2 and X3 are placed 2 cm below the left and right eye respectively. The amplifier links to the computer via USB. The measurements m_i for $i = 1, 2, \ldots, n$ are transmitted in packets covering time intervals of 0.2 sec, i.e. data packets are received by the controlling computer at a rate of 5 Hz. There is an additional delay of about 0.16 sec until the software that subscribed to the amplifier is notified that data is available.

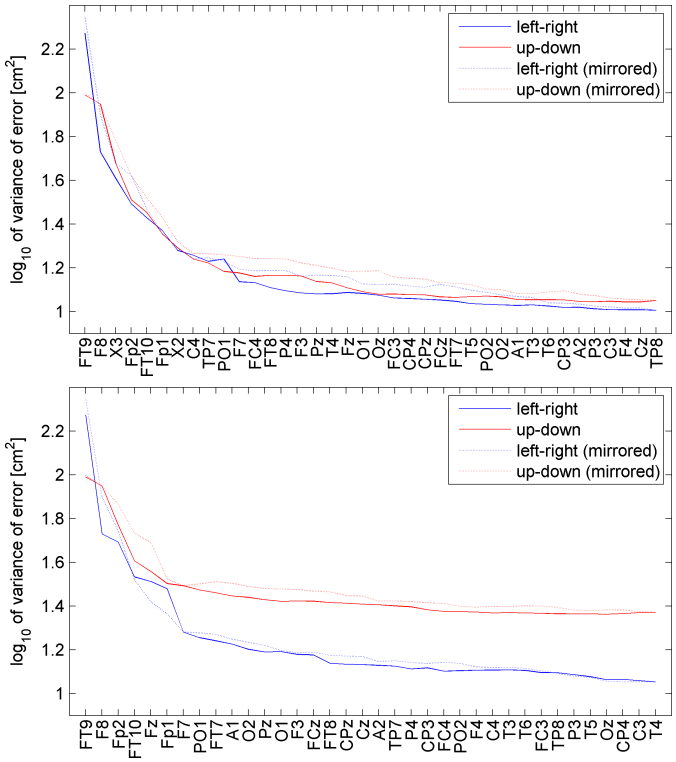

Fig. 6. Ordering of electrodes that minimize the maximum of horizontal and vertical estimation error obtained by greedy optimization. The dashed lines correspond to the ordering of electrodes mirrored along the centerline of the head for the purpose of comparison. *Top:* Electrodes X2 and X3 are connected 2 cm below the eyes. *Bottom:* No electrodes below the eyes.

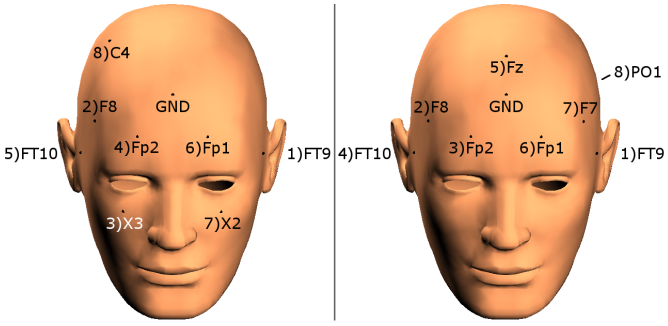

Fig. 7. Location of the 8 most significant electrodes on the head. *Left:* Electrodes X2 and X3 are connected 2 cm below the eyes. *Right:* No electrodes below the eyes.

B. Numerical evaluation

During calibration, each subject traces a moving cue with coordinates $p(t)$ on the screen over a period of $T = 2$ minutes while holding the head still. The curve $p(t)$ is displayed in Figure 2. The collected EEG data m_i for $i = 1, 2, \ldots, n$ is used to obtain the coefficients α_i^x, α_i^y for $i = 0, 1, 2, \ldots, n$ that minimize the squared error in (1). Shortly afterwards, the subject traces the moving cue $p(t)$ again. The EEG data m_i from the second pass together with the coefficients α_i^x, α_i^y are used to simulate the performance of the algorithm in Section II-C. The output of the algorithm is the estimated target of glance $\hat{p}'(t)$ in screen coordinates. We scale the difference $d(t) = p(t) - \hat{p}'(t) = (d^x(t), d^y(t))$ according to the actual

dimensions of the monitor to formulate the error in [cm] as

$$e(t) = (23.65 \cdot d^x(t), 14.85 \cdot d^y(t)) \tag{4}$$

The probability distribution of each coordinate of $e(t)$ averaged over 12 subjects is shown in Figure 5, the variances are listed in Table I individually. The correlation between horizontal and vertical approximation quality is significant. The standard deviation of the average error is less than 3.5 cm in each coordinate, which equivalents to 3.4 degrees of arc. The accuracy of glance estimation using traditional EOG equipment (six electrodes closely placed around the eyes) are stated for comparison: [15] reports a mean error of 1.8 degrees of arc horizontally, and 3.1 degrees vertically; [16] reports a mean deviation of ± 3.3 cm. These ratings serve as a guideline for the design of EOG controlled applications.

The estimation algorithm is defined for any subset of electrodes. Using the recordings described above, we simulate the accuracy of the estimation on subsets of electrodes. We investigate which electrodes are most valuable to simultaneously minimize the error in left-right and up-down glance. Using greedy optimization, we minimize

$$\sum_{j=1}^{12} \max\{\operatorname{var} e_j^x(t), \operatorname{var} e_j^y(t)\} \tag{5}$$

where $e_j(t)$ denotes the error function for subject $j = 1, 2, \ldots, 12$: starting with an empty subset of electrodes, each iteration we add the respective electrode that reduces (5) most. This process yields a priority list of electrodes, see Figure 6. For instance, if the system ought to run with 9 electrodes only, our evaluation suggests to connect FT9, F8, X3, Fp2, FT10, Fp1, X2, C4, and ground GND. The configuration may be mirrored along the centerline of the head without loss of precision.

TABLE I
VARIANCE OF ESTIMATION ERROR IN $[cm^2]$

	using X2, X3		without X2, X3	
subject id j	left-right	up-down	left-right	up-down
1	8.265	9.348	8.696	13.215
2	19.261	13.146	22.627	28.866
3	16.146	14.425	16.792	27.840
4	4.231	9.750	5.288	20.281
5	7.065	11.548	7.453	22.460
6	5.562	11.909	5.886	19.723
7	13.040	14.101	14.057	28.596
8	9.259	10.648	11.157	33.778
9	2.174	8.430	2.105	15.958
10	10.108	12.091	12.231	24.787
11	13.205	13.616	15.053	27.776
12	16.430	14.260	17.373	29.466
average	10.395	11.939	11.560	24.396

C. Benchmarks

Software to spell words is a popular benchmark among applications controlled by EOG [6, 7]. Our spelling software

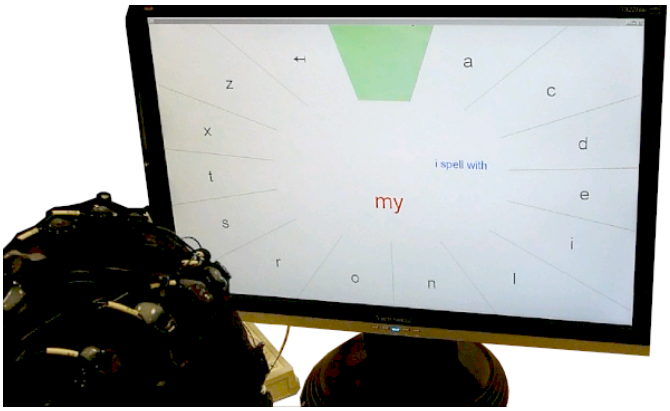

Fig. 8. Volunteer spelling a sentence using our English dictionary based spelling software - snapshot from [18].

demonstrates the reliability and convenience of our novel drift compensation. The letters of the English alphabet are aligned sequentially along an ellipse on the screen (see Figure 8). This alignment increases the probability that an offset in the estimation of glance due to drift resulting in a position outside of the screen, is corrected. In addition, our speller is dictionary based, which generally eases the selection of characters after the first few letters of a word have been spelled. Figures 4 exhibits the coordinates of $\hat{x}$ and $\hat{x}'$ for a sample trial. A calibration procedure of 1 minute duration preceedes the spelling.

In a recording of 27 minutes duration 358 characters (including spaces) were spelled. This is equivalent to 13.25 characters per minute with an accuracy of 100%. The average number of characters to choose from was $N = 17.4$, the average duration for a character selection was $T = 4.7$ seconds, and the selection was correct with a probability of $P = 0.98$. (Errors could be corrected by a backspace function.) In terms of the information rate derived from [17], the number of bits transferred per second were

$$\frac{1}{T}\left(\log_2 N + P\log_2 P + (1-P)\log_2 \frac{1-P}{N-1}\right) = 0.83\frac{\text{bits}}{\text{sec}}. \tag{6}$$

For comparison: The EOG controlled speller in [5] allows subjects to spell 5 letters in 24.7 sec with perfect accuracy. [6] report on spelling a sentence with 40 Japanese characters in 331.4 sec.

Another classic is the game *Breakout*, see Figure 3 and [18]: The game is about positioning a slider on the bottom of the screen to bounce off a ball. The control in our implementation relies only on the correct estimation of x-glance. To create an incentive for the subject to vary the glance along the x-axis and to reach the boundary of the screen, the ball never bounces off vertically. The gameplay consists only of a single state and is intuitive. Playing the game has been the favourite activity among the 12 volunteers who tested our EEG system. In a public demonstration of our system, a subject controlled the game for over 90 minutes with only few breaks and recalibrations in between.

IV. Conclusions

Previous EOG-based control schemes applied a high-pass filter to overcome the drift in the voltage measurements. Because the filter removes any constant offset, these schemes allow only for velocity control: rapid eye movements of the subject are recognized, but steady glance is not encoded. Therefore, EOG-based applications typically consist of a set of states. Transitions between the states occur when the subject oscillates the glance direction, or blinks [5, 6, 19]. However, fast oscillation of gaze direction, or frequent eye blinking is almost, but not quite, entirely unlike comfortable over an extended period of time.

In contrast, our algorithm does not filter the data. The subject controls the application by simply glancing at a target location on a computer screen, i.e. via position control. As a consequence, our applications use fewer states, and are more seamless to operate. The numerical evaluations and the performance of our benchmark applications suggests that control via glance direction is both more accurate and less exhausting than control via rapid eye gestures. The error in the position estimate is typically less than 5 cm in each coordinate.

Researchers have custom built EOG circuits, in order to reduce the cost and complexity of hardware [4, 5]. We look forward to learn about applying our algorithm on this specialized hardware.

[20] aims at the removal of eye artifact in EEG through the combination of EEG with an eye tracker to allow for single trials experiments. The mathematical model relates glance and eye artifacts in a 2nd order approximation, that is established by a Kalman filter. The method requires 20 to 30 seconds of calibration, that is followed by a period of 10 seconds of operation. The authors claim to yield better results than PCA, or SOBI. The authors report that the parameters of the Kalman filter have to be preselected in order to converge. The glance estimation presented in this paper has a smaller calibration-to-operation ratio and is numerically stable. In the future, we hope to show that our algorithm benefits the removal of eye artifacts from EEG.

References

[1] R. Barea, L. Boquete, M. Mazo, and E. Lopez, *System for Assisted Mobility Using Eye Movements Based on Electrooculography*, IEEE Transactions on Neural Systems and Rehabilitation Engineering, vol. 10, no. 4, pp. 209-218, 2002

[2] M. Ebeling, *The invention that unlocked a locked-in artist*, http://tinyurl.com/42pg8wb, TEDActive, March 2011

[3] Y. Chen and Y. Newman, *A Human-Robot Interface Based on Electrooculography*, Proceedings of the IEEE International Conference on Robotics and Automation, pp. 243-248, April 2004

[4] S. Venkataramanan, P. Prabhat, S. Choudhury, H. Nemade, and J. Sahambi, *Biomedical Instrumentation based on Electrooculogram Signal Processing and Application to a Hospital Alarm System*, Proceedings of the 2nd IEEE International Conference on Intelligent Sensing and Information Processing, pp. 535-540, January 2005

[5] A. Usakli, S. Gurkan, F. Aloise, G. Vecchiato, and F. Babiloni, *On the Use of Electrooculogram for Efficient Human Computer Interfaces*, Computational Intelligence and Neuroscience, 2010

[6] H. Tamura, M. Miyashita, K. Tanno, and Y. Fuse, *Mouse Cursor Control System using Electrooculogram Signals*, World Automation Congress, 2010

[7] A. Usakli and S. Gurkan, *Design of a Novel Efficient Human-Computer Interface: An Electrooculagram Based Virtual Keyboard*, IEEE Transactions on Instrumentation and Measurement, vol. 59, no. 8, pp. 2099-2108, August 2010

[8] C. Hsieh, H. Chen and T. Jong, *The Study of the Relationship between Electro-oculogram and the Features of Closed Eye Motion*, Proceedings of the 5th International Conference on Information Technology and Application in Biomedicine, May 2008

[9] M. Fatourechi, A. Bashashati, R. Ward, and G. Birch, *EMG and EOG artifacts in brain computer interface systems: A survey*, Clinical Neurophysiology 118, pp. 480-494, 2007

[10] R. Barea, L. Boquete, M. Mazo, E. Lopez and L. Bergasa, *E.O.G. Guidance of a Wheelchair using Neural Networks*, International Conference on Pattern Recognition, vol. 4, 2000

[11] L. Geddes, J. Bourland, G. Wise, and R. Steinberg, *Linearity of the Horizontal Component of the Electro-oculogram*, Medical and Biological Engineering, pp. 73-77, January 1973

[12] D. Kumar and E. Poole, *Classification of EOG for Human Computer Interface*, Proceedings of the 2nd Joint IEEE Annual International Conference of the Engineering in Medicine and Biology Jointly with the 24th Annual Conference of the Biomedical Engineering Society, vol. 1, pp. 64-67, October 2002

[13] Y. Kim, N. Doh, Y. Youm, and W. Chung, *Development of Human-mobile Communication System using ElectroOculoGram Signals*, International Conference on Intelligent Robots and Systems, pp. 2160-2165, 2001

[14] J. Hakenberg, W. Lee, T. Tan, A. Mansour, and C. Guan, *A new paradigm to quantify the manifestation of eye movements in the electroencephalogram*, Proceedings of the Engineering and Physical Sciences in Medicine and the Australian Biomedical Engineering Conference, December 2010

[15] J. Woestenburg, M. Verbaten, and J. Slangen, *Eye-movements in a two-dimensional plane: a method for calibration and analysis using the vertical and horizontal EOG*, Biological Psychology, vol. 18, pp. 149-160, March 1984

[16] X. Zhang, T. Sugi, X. Wang, and M. Nakamura, *Real-time estimation system of the gaze position based on an electrooculogram*, Artificial Life Robotics, vol. 14, pp. 182-185, 2009

[17] C. Shannon, and W. Weaver, *The Mathematical Theory of Communication*, The University of Illinois Press, 1964

[18] J. Hakenberg, *Applications of the NuAmps Digital EEG Amplifier*, http://www.hakenberg.de/automation/neuroscan_nuamps.htm, March 2011

[19] M. Trikha, A. Bhandari, and T. Gandhi, *Automatic Electrooculogram Classification for Microcontroller Based Interface Design*, Systems and Information Engineering Design Symposium, 2007

[20] J. Kierkels, J. Riani and J. Bergmans, *Using an Eye Tracker for Accurate Eye Movement Artifact Correction*, IEEE Transactions on Biomedical Engineering, vol. 54, no 7, 2007